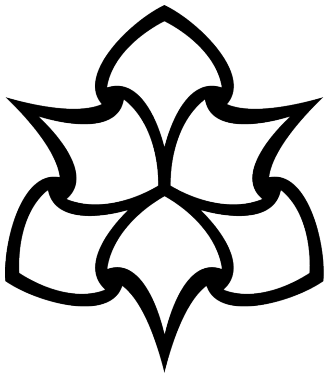

Multi-Renewable Energy Agent Based Control for Economic Dispatch and Frequency Regulation of Autonomous Renewable Grid

F. Mehmood[1], B. Khan[1], S. M. Ali[1], B. Qureshi[1], C. Diver[2], and R. Nawaz[2]
[1]Department of Electrical Engineering, CUI Abbottabad Campus, Pakistan
[2]Manchester Metropolitan University, Manchester, UK

Corresponding author: M. B. Qureshi (e-mail: bilalqureshi@cuiatd.edu.pk).

ABSTRACT This paper addresses frequency regulation and the economic dispatch problem of an Autonomous Renewable Grid (ARG) primarily composed of Multi Renewable Energy Agents (MRAs), interfaced through DC/AC inverters. A large number of MRAs that have an inherent fluctuating nature and frequent disturbances in inter-connected systems require fast and robust control to stabilize the frequency and to maintain cost-effective operation of an ARG. To address the above control challenges, Distributed Averaging Integrator (DAI) based control schemes were proposed in various research works. The main flaws of such schemes were slow convergence, sluggish response, poor transient performance and a difficult selection of an appropriate damping-factor. The proposed approach introduces a Distributed Sliding Mode Control (DSMC) based solution for fast convergence and improved transient response. The DSMC control is based on a distributed sliding surface, designed using a combination of local information and information from neighboring MRAs. The control is implemented locally at each MRA and achieves the asymptotic global consensus. Finally, the convergence of the proposed control scheme is proved mathematically, and performance is validated using the MRA system which has been implemented using MATLAB/Simulink. The results of the proposed control technique are compared with conventional DAI control, which shows that the proposed scheme outperforms the conventional scheme in terms of fast convergence, considering renewable resources as distributed generation.

INDEX TERMS Distributed SMC, Secondary Control, Frequency Regulation, Distributed Generation, Renewable Grid, System Stability.

I. INTRODUCTION

The Autonomous Renewable Grid (ARG) is primarily composed of inverter-interfaced Multi-Renewable Agents (MRAs)/Distributed Generation [1], [2]. The increased number of MRAs is challenging the successful operation of the ARG due to their low inertia [3]. Due to the intermittent nature of MRA's as well as their widely distributed geographical nature, small capacity and the large number of them they demand a fast and robust distributed control system for frequency regulation and economically optimized power production. The Distributed Averaging Integrator (DAI) based control schemes proposed in contemporary research work exhibit a slow response especially in providing Economic Dispatch (ED). This paper proposes Distributed Cooperative Sliding Mode Control (DCSMC) to comply with the control demands of an ARG.

Unlike large synchronous generators with constant 50/60 Hz frequency, MRAs either produce power in the form of DC (PV plants, fuel cells, and storage batteries) or variable speed AC (wind and micro-turbines). In both cases a DC to AC inverter is required to connect to the wider AC network [4]. Moreover, the large synchronous generators possess inherent synchronization capabilities, while the MRAs rely on their associated control to achieve synchronization [5], [6].

The conventional approach to address the aforementioned control challenges is to divide it into four main categories namely; *inner-control, primary, secondary* and *tertiary* control [7], [8]. The *inner-control* is the local control of the inverter that provides the current, voltage, output impedance regulation, and synchronization with the grid. *Inner-control* provides high frequency switching pulses for the inverter to produces the sinusoidal voltage of desired phase/frequency and amplitude. The *primary* control uses a proportional droop-control technique to provide active and reactive power sharing among the MRAs but forces the frequency and

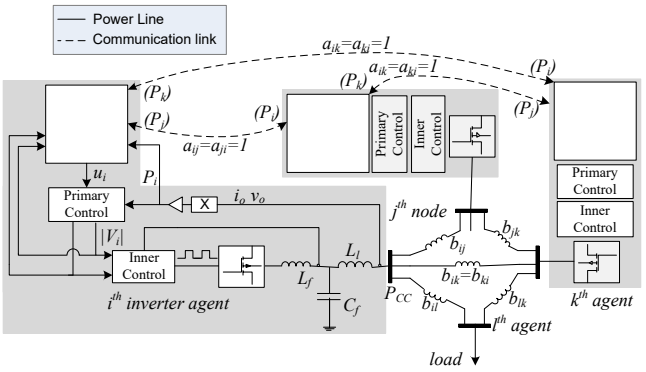

Figure 1. Hierarchical control structure of inverter and inter-MRA power lines

voltage to deviate from their nominal values [9], [10]. This naturally requires an additional layer of control; the *secondary* control, to minimize the deviations produced by the primary control. The ED is provided by *tertiary* control that forces the MRAs to follow the optimum power injection profiles for cost effective operation of the system. However, recent research has merged the *tertiary* control into the *secondary* control, providing ED and frequency regulation at the same level [11-13].

Figure 1 represents the inverter with associated hierarchical control architecture and inter-MRA connection through power lines and communication links. The susceptance of the power line connecting the i^{th} and j^{th} MRAs, is labelled as b_{ij} $(b_{ij} = b_{ji})$. The *secondary* and *tertiary* controls require the power feedback from local and neighboring MRAs to generate the control input for frequency stabilization and ED. The information from neighboring MRAs is obtained through inter-MRA communication links. Based on the control input from *secondary* control, the *primary* control generates the reference values of frequency and voltage for *inner control*. The *inner control* works on a faster scale to provide synchronization with the grid system and tracks the reference values from the *primary* control by producing appropriate gate pulses for the inverter.

The *secondary* (and *tertiary*) control of MRAs could be centralized [14], [15], decentralized [16], [17] as well as distributed [11-13], [18], [19]. The centralized control provides frequency regulation and ED, with the help of communication links with individual MRAs. The communication links are used to obtain the information about frequency and local power generation and transmits the control input to the MRAs. Similarly, in distributed control, MRA units develop a co-operative control with the help of peer-to-peer communication links between the MRAs, while the decentralized control is a local control without any communication link. However, the distributed control which provides the flexibility of a plug-and-play feature as the number of MRAs increases has gained significant attention recently, especially in case of ARG [12], [13]. In centralized control a single communication link failure results in isolation/disconnection of an MRA and may compromise the frequency regulation of the system. However, in distributed control, multiple communication paths can exist in the network and failure of communication link/links would not affect the overall performance as long as the MRAs form a connected graph with active communication links.

A variety of distributed *secondary* control solutions were proposed in recent research and extensively discussed, among them is the DAI (or Distributed Averaging Proportional Integrator (DAPI)). The DAI based control schemes were proposed for bulk-hybrid power systems [20], [21] as well as for microgrids [10], [12], [22]. The author in [23] introduced the distributed averaging filter technique where the agents achieved a common consensus throughout the network with the help of communication links. The work formed the basis for different averaging-based techniques. The author in [21], proposed the distributed proportional integral for bulk power system, while the author in [22] presented the same technique for medium voltage, MG, with slight modifications to provide proportional power sharing. The optimum resource allocation criterion was developed in [12] and implemented using the DAI control technique for heterogeneous power systems. Detailed analysis of DAI with stability analysis in the presence of communication delays, link failures and dynamic network topologies was presented in [13]. The author in [24] discussed the performance limitation and problematic tuning of DAI.

The DAI control is based on the integration of local state-errors and weighted-summation of inter-MRA state-errors. The inter-MRA state-errors are formed with the help of communication links. The prime short-coming of DAI control is the slow response, especially, in minimizing the inter-MRA state-errors.

The MRA based ARG experiences frequent changes in real power consumption, perturbations and MRA intermittence causing imbalance of real power, resulting in frequency deviation [25], [26]. Under such conditions, consensus development for ED becomes an even more challenging task, thus demanding a fast and robust cooperative control for low inertia ARG.

This research work focuses on the frequency stabilization and optimum resource allocation aspect of *secondary* control and proposes a novel DCSMC scheme. It is the foremost attempt to design DSMC based *secondary* control. The proposed (DCSMC) adds the robustness and fast convergence attributes of Sliding Mode Control to the *secondary* control resulting in improved stability and better transient response for the ARG. The main contributions of this paper are listed below;

- In this paper, we propose a DCSMC for MRA based ARG. The control is implemented in a distributed manner at each MRA and creates a global consensus

throughout the network with the help of communication links between the MRAs.

- Our proposed work provides fast and robust convergence in frequency regulation and ED. The control maintains the real power balance to regulate the frequency and utilizes the identical incremental cost criteria for ED.
- We provide rigorous mathematical proof of the proposed control scheme using Lyapunov Candidate Function.
- In order to critically investigate the performance of DCSMC, a 'seven' node system is designed and evaluated in MATLAB/Simulink that validates our control performance, compared to prior works.

The paper is organized as follows; Section 2 starts with, an introduction to various Notations, Graph Theory and a mathematical model of inverter-based ARG. The section also contains control objectives and a brief introduction of a DAI control technique. Section 3 presents the design of a distributed sliding surface for DCSMC. The stability and convergence proof are discussed in Section 4. Section 5 presents the performance analysis and comparison with DAI control using a MATLAB/Simulink based model. Conclusions and future work are presented in Section 6.

II. Mathematical Model of ARG

This section discusses the primary control dynamics and control objectives for secondary control. The section also presents a brief introduction of DAI control. The section starts with nomenclature, an introduction to the various notations used in the paper and graph theory.

A. Nomenclature

The scalar parameters are related to individual MRAs, while the vector/matrix form represents the whole network.

Scalar Value	Vector/Matrix Form	Description
$\theta_i \in \mathbb{R}$	$\theta \coloneqq col(\theta_i) \in \mathbb{R}^{\mathbb{a}_P \times 1}$	Voltage phase angle
$\omega_i \in \mathbb{R}$	$\omega \coloneqq col(\omega_i) \in \mathbb{R}^{\mathbb{a}_P \times 1}$	Angular frequency
$\omega_d \in \mathbb{R}_{>0}$		Nominal Frequency
$m_i \in \mathbb{R}_{>0}$	$M \coloneqq diag(m_i) \in \mathbb{R}^{\mathbb{a}_P \times \mathbb{a}_P}$	(virtual) Inertia of MRA
$d_i \in \mathbb{R}_{>0}$	$D = diag(d_i) \in \mathbb{R}^{\mathbb{a}_P \times \mathbb{a}_P}$	Damping coefficient
$p_i \in \mathbb{R}_{>0}$	$P \coloneqq col(p_i) \in \mathbb{R}^{N_\mathbb{a} \times 1}$	Power production of MRA
$p_i^d \in \mathbb{R}_{\geq 0}$		Power set point
$u_i \in \mathbb{R}$	$u \coloneqq col(u_i) \in \mathbb{R}^{N_\mathbb{a} \times 1}$	Control input (provided by *secondary* control)
$p_{\mathbb{a},i} \in \mathbb{R}$	$P_n \coloneqq col(p_{\mathbb{a},i}) \in \mathbb{R}^{N_\mathbb{a} \times 1}$	Power flow to neighboring MRAs
$p_{LL,i} \in \mathbb{R}_{\geq 0}$	$P_{LL} \coloneqq col(p_{LL,i}) \in \mathbb{R}^{N_\mathbb{a} \times 1}$	Local load at MRA
$v_i \in \mathbb{R}_{>0}$		Voltage amplitude
$b_{ij} \in \mathbb{R}_{\geq 0}$		Susceptance between i^{th} and j^{th} MRAs
$g_i \in \mathbb{R}_{\geq 0}$		Conductance of local load
$p_{l,i} \in \mathbb{R}_{\geq 0}$	$L \coloneqq col(p_{l,i}) \in \mathbb{R}^{n_L \times 1}$	Power absorption of load-units
$c_i \in \mathbb{R}_{>0}$	$C = diag(c_i) \in \mathbb{R}^{N_\mathbb{a} \times N_\mathbb{a}}$	Production Cost-rate of MRA
k_w & $k_p \in \mathbb{R}_{>0}$		Tuning parameters of DAI

B. Notations

Let X_1 and X_2, be the set of elements and notation $X_{1\cap 2}$, denotes the set of elements $\{x|\, x \in X_1 \cap X_2\}$. While X_{1-2}, denotes the set of elements $\{x|x \in X_1 - X_2\}$. The cardinality of a set X is denoted by $|X|$. Let $\mathbb{0}$, denote a null set, $\mathbb{R}$ denote the set of real numbers and the notation $\mathbb{R}_{\geq 0}$, denotes a set $\{x \in \mathbb{R} | x \geq 0\}$, and $\mathbb{R}_{>0} \coloneqq \{x \in \mathbb{R} | x > 0\}$. $x \coloneqq col(x_i) \in \mathbb{R}^{n\times 1}, i = 1, \dots, n$, represents the elements x_i as a column matrix of length n. $\mathbf{1_n} \in \mathbb{R}^{n\times 1}$ denotes a column matrix of ones and $I_n \in \mathbb{R}^{n\times n}$ is an identity matrix. The $X = diag(x_i) \in \mathbb{R}^{n\times n}$, denotes a diagonal matrix, with x_i as the diagonal elements. For a matrix $X \in \mathbb{R}^{n\times n}, X > 0$ indicates that X is a positive definite matrix, while $X < 0$ indicates that X is a negative definite matrix.

C. Graph Theory

Let $\mathcal{G}$ be a static, undirected and connected graph with $N = \{1, \dots n\}$, representing the set of nodes and $E \in N \times N$, representing the set of edges. The adjacency matrix of $\mathcal{G}$ is represented by a symmetric matrix; $A \in \mathbb{R}^{n\times n}$ with elements $a_{ij} = a_{ji} = 1$, if the MRAs are connected directly by an edge and $a_{ij} = a_{ji} = 0$, otherwise. The degree matrix of $\mathcal{G}$ is defined as $\mathbb{Q} = diag(\mathbb{d}_i) \in \mathbb{R}^{n\times n}$, where $\mathbb{d}_i = \sum_{j=1}^{n} a_{ij}$. The Laplacian matrix $\mathcal{L}$, of $\mathcal{G}$ is defined as $\mathcal{L} = \mathbb{Q} - A, \in \mathbb{R}^{n\times n}$.

D. Power Network

We consider a power network represented by a graph $\mathcal{G}$ with n nodes. The nodes in $\mathcal{G}$ are categorized as; MRAs and load-units. MRAs possess a distributed renewable energy source (DG) with an optional local-load. The set of MRAs is represented by $N_\mathbb{a} = \{1, \dots . n_\mathbb{a}\}$, while the set of load-units is represented as $N_L = \{n_\mathbb{a} + 1, \dots, n_\mathbb{a} + n_L\}$, such that $\mathrm{N} = \{N_\mathbb{a} \cup N_L\}$ $(n = n_\mathbb{a} + n_L)$. The load-units consists of active power loads. $\mathcal{G}$ is connected in terms of power lines (as shown in Figure 1) and for simplicity we assume that the power lines are purely inductive and a susceptance $b_{ij} > 0$, $i,j \in N$, if a power line exists between the i^{th} and j^{th} MRAs and $b_{ij} = 0$ represents the absence of power line. The set of neighboring

MRAs of i^{th} MRA are defined as $N_{b,i} = \{n_j \in N | b_{ij} \neq 0\}$. The communication links in the network are represented by an Adjacency Matrix (A_c). The presence of a communication link between i^{th} and j^{th} MRAs is indicated by the corresponding element of the Adjacency Matrix as; $a_{ij} = a_{ji} = 1$, while the absence of a link is represented by $a_{ij} = a_{ji} = 0$. The associated Laplacian Mtrix is represented by $\mathcal{L}$. The set of neighboring MRAs of i^{th} MRA, in terms of communication links, is defined as $N_{c,i} = \{n_j \in N_{\text{a}} | a_{ij} \neq 0\}$.

Assumption 1: For simplicity, we assume the MRAs are connected through pure inductive power lines, so the real power loss in the power lines is zero. The voltage magnitude on each MRA is assumed to be 1 pu.

Assumption 2: MRAs are equipped with power and phase measurement units.

Power measurement is an integral part of conventional hierarchical control as shown in Figure 1, while instantaneous phase can be extracted from associated inner-control of inverter-interfaced MRA units.

Assumption 3: For each MRA, we have two different types of neighboring MRAs; $N_{a,i}$ and $N_{b,i}$, and we relax the condition of identical power and communication neighbors, instead we assume that for i^{th}, MRA $N_{c\cap b,i} = \{N_{c,i} \cap N_{b,i}\} \notin \mathbb{O}, i \in N_p$

We consider the real power loads and inverter-interfaced MRA, with primary control emulating the behavior of a synchronous generator [8], [10], [11]. The dynamics of i^{th} MRA ($i \in N_{\text{a}}$) is given by,

$$\begin{aligned} \dot{\theta}_i &= \omega_i, \\ m_i\dot{\omega}_i + d_i(\omega_i - \omega_d) + p_i^d + p_i &= u_i. \end{aligned} \tag{1}$$

In the case of inverter interfaced MRA, the virtual inertia $m_i = \tau_i d_i$, where $\tau_i \in \mathbb{R}_{>0}$ represents the time constant of low pass filter for power measurement [13]. Without loss of generality, the power set point p_i^d is set to zero. The power produced by the MRA (p_i) is given by,

$$p_i = p_{\text{a},i} + p_{LL,i}, \quad i \in N_{\text{a}}. \tag{2}$$

Where, $p_{\text{a}.i}$ is the power flow to neighboring MRAs, while $p_{LL,i}$ is the power flow to local-load.

$$\begin{aligned} p_{\text{a},i} &= \textstyle\sum_{j\in N_{b,i}} b_{ij} v_i v_j \sin(\theta_i - \theta_j), \\ p_{LL,i} &= v_i^2 g_i. \end{aligned} \tag{3}$$

While the dynamics of i^{th} load-unit is given by,

$$p_{l,i} + \textstyle\sum_{j\in N_{b,i}} b_{ij} v_i v_j \sin(\theta_i - \theta_j) = 0, \qquad i \in N_L. \tag{4}$$

Where, $p_{l,i}$ is the real power consumption of the load-unit. Now, the dynamics of MRAs can be represented compactly in matrix form as,

$$\begin{aligned} \dot{\theta} &= \omega, \\ M\dot{\omega} + D\big(\omega - \mathbf{1}_{n_P}\omega_d\big) + P_n + P_{LL} &= u, \end{aligned} \tag{5}$$

While the load-units are represented as,

$$L + \tilde{L} = 0. \tag{6}$$

Where, $\tilde{L} = col\Big(\sum_{j\in N_{b,i}} b_{ij} v_i v_j \sin(\theta_i - \theta_j) = 0\Big) \in \mathbb{R}^{n_L \times 1}$, $i \in N_L$.

Now, from the dynamics of the ARG in (1) and (4), the system would operate at nominal frequency only when,

$$u_i = p_{LL,i} + p_{\text{a},i}. \tag{7}$$

While, for the complete network the frequency regulation would be achieved when,

$$\mathbf{1}_{n_L}^T L = \mathbf{1}_{n_{\text{a}}}^T P_n. \tag{8}$$

Equation (8) holds because of Assumption 1 which considers a lossless ARG model where, the sum of power delivered to the neighboring nodes is equal to the sum of power consumed by the load nodes.

E. Control Objectives

The control objectives for the *secondary* control are, to regulate the frequency to its nominal value (ω_d) and to provide ED. It is clear from (8) that frequency regulation depends upon the balance of real power. The criterion for optimum power production is based on identical incremental cost [12]. So, the control objectives can be written as,

$$\text{a.} \quad \omega_i - \omega_d = 0, \qquad \forall i \in N_{\text{a}}, \tag{9}$$

$$\text{b.} \quad c_i u_i - c_j u_j = 0, \qquad \forall i, j \in N_{\text{a}}. \tag{10}$$

Frequency regulation of the system is represented in (9), while (10) represents the criteria for ED. The system would operate at optimum cost when the incremental cost ($c_i u_i$) is identical for a complete network. The system reaches equilibrium when it satisfies the control objectives in (9) and (10) simultaneously for all MRAs.

F. Distributed Averaging Integral based Secondary Control

DAI based *secondary* control uses peer-to-peer communication between the nearby neighboring MRAs to create the consensus in the network. The control is based on integration of error in (9) and (10). The control law DAI is given by,

$$\dot{u}_i = -k_w(\omega_i - \omega_d) - k_p \textstyle\sum_{j\in N_{c,i}} (c_i u_i - c_j u_j), i \in N_{\text{a}} \tag{11}$$

Where, k_w and k_p represents the weight on error in (9) and (10), respectively. The control objective in (10) is based on consensus to identical incremental cost, for the complete network. However, control law in (11) uses neighboring communication set ($N_{c,i}$) to form the error.

The control law in (11) is implemented locally at each MRA and creates consensus throughout the network. The control law in (11) provides active frequency regulation but possesses slow convergence to identical cost. In the presence of an increased number of small-scale MRA units with fluctuating outputs and frequent disturbances in the system, the DAI based *secondary* control would become ineffective.

III. Distributed Cooperative Sliding Mode Control

DCSMC is proposed in the work for fast convergence, effectively complying with the control requirements of ARG. The design of DCSMC possesses two essential parts; distributed sliding surface design and reaching law design. Firstly, an intermediate local sliding surface is designed based on state-errors, then distributed sliding surface is designed using weighted summation of local and neighboring intermediate sliding surfaces. The control law forces the system trajectories to asymptotically converge to the distributed sliding surface.

For ease of formulation, we start with translating the dynamics in (5) into deviation variables. Let, $\Delta\omega = \omega - \omega_d$ and $\Delta\theta = \theta - \omega_d t$. So, (5) becomes,

$$\begin{aligned} \Delta\dot{\theta} &= \Delta\omega, \\ M\Delta\dot{\omega} + D\Delta\omega + P &= u. \end{aligned} \tag{12}$$

Let, $\chi_i = [\Delta\theta_i \ \Delta\omega_i]^T \in \mathbb{R}^{2\times 1}$ collectively represent the states in (12) and $\chi_i^* = [\Delta\theta_i^* \ \Delta\omega_i^*]^T \in \mathbb{R}^{2\times 1}$ represents the optimum or the equilibrium value. The optimum state χ_i^* is defined to satisfy the control objective in (9) and (10) simultaneously. From (9), $\Delta\omega_i^* = 0$, the equilibrium value of angular frequency is the same for each MRA ($\omega_i^* = \omega_d$). Now, the equilibrium information of $\Delta\theta_i^*$ should be obtained using (10). Using the same technique of near-neighbor communication adopted in (11), (10) can be represented as:

$$\sum_{j=1}^{n_{\mathbb{a}}} a_{ij}(c_i u_i - c_j u_j) = 0, \quad i \in N_{\mathbb{a}}. \tag{13}$$

Here, a_{ij} is used to represent the neighboring communication set $N_{c,i}$. Now, rewriting (13) using the result in (7) and then representing it in matrix form. Note that, (7) is based on nominal operational frequency of the system.

$$\sum_{j=1}^{n_{\mathbb{a}}} a_{ij}\left(c_i p_i - c_j p_j\right) = 0, \qquad i \in N_{\mathbb{a}}, \tag{14}$$

$$\mathcal{L}CP = 0. \tag{15}$$

Remark 1: Equation (15) does not possess a unique solution in terms of $\Delta\theta$, as C is the positive-definite diagonal matrix, while the Laplacian matrix $\mathcal{L} \in \mathbb{R}^{n_{\mathbb{a}}\times n_{\mathbb{a}}}$ has a rank equal to $n_{\mathbb{a}} - 1$ [27].

Since the global equilibrium value $\Delta\theta_i^*$ is not available, each MRA finds a local intermediate-optimum state value $\tilde{\chi}_i^* = [\Delta\tilde{\theta}_i^* \ \Delta\tilde{\omega}_i^*]^T \in \mathbb{R}^{2\times 1}$ where $\Delta\tilde{\omega}_i^* = 0$. $\tilde{\chi}_i^*$ is calculated with the help of local and neighboring information, and locally satisfies the control objectives in (9) and (10). Now for $\Delta\tilde{\theta}_i^*$, we represent (14) using (2),

$$p_{\mathbb{a},i} = \frac{1}{|N_{c,i}|c_i}\sum_{j\in N_{c,i}}\{c_j p_j\} - p_{LL,i}. \tag{16}$$

Now, rewriting (16) using Assumption 3 to divide the neighboring set $N_{c,i}$ into $N_{a\cap b,i}$; the neighboring MRAs with both the communication and power links d $N_{b-c,i}$; the neighboring MRAs with power link but no communication.

$$\sum_{j\in N_{b\cap c,i}} b_{ij}v_i v_j \sin\left(\Delta\tilde{\theta}_i^* - \Delta\theta_j\right) = \frac{1}{|N_{c,i}|c_i}\left\{\sum_{j\in N_{ai}}\{c_j(p_j)\} - p_{LL,i}\right\} - \acute{p}_i, \tag{17}$$

Where, $\acute{p}_i = \sum_{j\in N_{b-c,i}} b_{ij}v_i v_j \sin\left(\Delta\tilde{\theta}_i^* - \Delta\theta_j\right)$. The value of power ($p_j$) and phase deviation ($\Delta\theta_j$) of neighboring MRAs are obtained through communication links, while $p_{LL,i}$ and $\acute{p}_i$ are measured locally. The value of desired phase deviation for i^{th} MRA ($\Delta\tilde{\theta}_i^*$) can be calculated as,

$$\Delta\tilde{\theta}_i^* = sin^{-1}\left\{\frac{k_i}{\sqrt{{x_i}^2+{y_i}^2}}\right\} - tan^{-1}\left(\frac{y_i}{x_i}\right), \tag{18}$$

Where, $k_i = \frac{1}{|N_{c,i}|c_i}\left\{\sum_{j\in N_{c,i}} c_j p_j - p_{LL,i}\right\} - \acute{p}_i$, $x_i = \sum_{j\in N_{b\cap c,i}} b_{ij}v_i v_j \cos(\Delta\theta_j)$ and $y_i = \sum_{j\in N_{b\cap c,i}} b_{ij}v_i v_j \sin(\Delta\theta_j)$.

Remark 2: It is clear from the derivation of (18) that the intermediate-optimum point $\Delta\tilde{\theta}_i^*$ simultaneously satisfies the objectives in (9) and (10), locally at each MRA. Tracking the intermediate-optimum state $\tilde{\chi}_i^*$ would lead χ_i to a global optimum point χ_i^* (the proof is discussed in Section 4).

Now, the control objectives in (9) and (10) transform to;

$$\chi_i - \tilde{\chi}_i^* = 0, \ \ \forall i \in N_{\mathbb{a}}, \tag{19}$$

Remark 3: The global equilibrium would be achieved if (19) is satisfied simultaneously for the complete network, that is, if $\chi - \tilde{\chi}^* = 0$, then $\chi = \chi^*$, where $\chi = col(\chi_i) \in \mathbb{R}^{2n_{\mathbb{a}}\times 1}$.

The intermediate sliding surface is designed based on state-error with intermediate optimum phase value in (19); $e_{1,i} = \Delta\theta_i - \Delta\tilde{\theta}_i^*$, and $e_{2,i} = \Delta\omega_i$. Now using Lyapunov design,

$$\Delta\omega_i = -\lambda\left(\Delta\theta_i - \Delta\tilde{\theta}_i^*\right). \tag{20}$$

Where $\lambda \in \mathbb{R}_{>0}$ is constant. The intermediate sliding surface is given by,

$$\mathcal{s}_i = e_{2,i} + \lambda e_{1,i}. \tag{21}$$

The sliding surface is the combination of local and neighboring intermediate sliding surfaces [28].

$$s_i = \sum_{j\in N_{c,i}} a_{ij}(\mathcal{s}_i - \mathcal{s}_j) + \mathcal{s}_i, \qquad i \in N_{\mathbb{a}}.$$

Where, $\mathcal{s}_j$ represents the sliding surfaces of neighboring MRAs, obtained through communication links. The sliding surface for complete system can be represented in matrix form as,

$$S = \begin{bmatrix} s_1 \\ \vdots \\ s_{n_{\mathbb{a}}} \end{bmatrix} = (\mathcal{L} + I)\begin{bmatrix} \mathcal{s}_i \\ \vdots \\ \mathcal{s}_{n_{\mathbb{a}}} \end{bmatrix}. \tag{22}$$

The reaching law for individual MRAs is designed as,

$$\dot{s}_i = -\psi\left(\sum_{j\in N_{c,i}} a_{ij}\left(s_i - s_j\right) + s_i\right) - \varphi\left(\sum_{j\in N_{c,i}} a_{ij}\left(sgn(s_i) - sgn(s_j)\right) + sgn(s_i)\right).$$

Where ψ and φ are tuning parameters. In matrix form the above equation be represented as,

$$\dot{S} = -(\mathcal{L} + I)\left(\psi S + \varphi sgn(S)\right). \tag{23}$$

Comparing (22) and (23),

$$\dot{s}_i = -\psi s_i - \varphi sgn(s_i). \quad (24)$$

From (21),

$$\dot{s}_i = \Delta\dot{\omega}_i + \lambda\Delta\omega_i - \lambda\Delta\dot{\tilde{\theta}}_i^*. \quad (25)$$

Using (12), (24) and (25), the control law for individual MRAs is given by,

$$u_i = -m_i\{\psi s_i + \varphi sgn(s_i)\} + (d_i - \lambda m_i)\Delta\omega_i + p_i + m_i\lambda\Delta\dot{\tilde{\theta}}_i^*. \quad (26)$$

Remark 4 (Chattering Effect): The *secondary* control, in the proposed control strategy, is based on control law (26), containing chattering effect. However, the second order dynamics of *primary* control (12) smooths-out the fluctuations in the control law. Moreover, a low-pass filter is also present with each inverter to remove the harmonics produced due to high frequency switching in *inner* control.

Remark 5: The proposed control is designed to provide fast and robust convergence for low inertia MG. However, following the contemporary *secondary* control solutions, the dynamics of inner-control, inverter, low pass filter and delays in communication links are not modelled.

IV. Stability Analysis

The stability analysis comprises the stability proof of reaching phase and sliding phase. The stability of the former is proved using Lyapunov function, while stability of sliding phase is intuitively obvious. Now, the following Lemma would be helpful in stability proof.

Lemma 1: The sum of Laplacian matrix; $\mathcal{L} \in \mathbb{R}^{n_{\mathbb{a}} \times n_{\mathbb{a}}}$, corresponding to connected communication graph of MRAs and Identity matrix $I_{n_{\mathbb{a}}}$, is positive definite ($\mathcal{L} + I_{n_{\mathbb{a}}} > 0$).

Proof: The proof of lemma is similar to the ones used for the sum of Laplacian matrix and pinning matrix in [27]. ■

A. Reaching Phase

Theorem 1: Consider the system represented in (12) and DCSMC based control law in (26) with $\psi > 0$, $\varphi > 0$ and $\lambda > 0$, then the sliding phase, that is $S = 0$ would be reached in a finite duration (t) with upper bound $t < \frac{\|S(0)\|_2}{\varphi\sigma_{min}}$, where σ_{min} represents the smallest eigen value of $\mathcal{L} + I_{n_{\mathbb{a}}}$.

Proof: Consider Lyapunov Candidate Function as [28],

$$V = \frac{1}{2}S^T S.$$

Taking the derivative of Lyapunov Candidate Function

$$\dot{V} = -S^T(\mathcal{L} + I_{n_{\mathbb{a}}})\psi S - S^T(\mathcal{L} + I_{n_{\mathbb{a}}})\varphi sgn(S), \quad (27)$$

Since $(\mathcal{L} + I_{n_{\mathbb{a}}}) > 0$, so the first term on R.H.S of (21) is negative definite, now using $sgn(S) \geq \frac{S}{\|S\|_2}$, we can write,

$$\dot{V} \leq \frac{-S^T(\mathcal{L}+I_{n_{\mathbb{a}}})(\varphi S)}{\|S\|_2}. \quad (28)$$

Hence $\dot{V}$ is negative definite, now using Rayleigh's Quotient, we can rewrite (28) as,

$$\dot{V} \leq -\sigma_{min}\varphi\|S\|_2. \quad (29)$$

To derive the convergence time, the Lyapunov Candidate Function can be rewritten as $V = \frac{1}{2}\|S\|_2^2$. Now, comparing the derivative of Lyapunov Function with (29) we get,

$$\|\dot{S}\|_2 \leq -\varphi\sigma_{min} \quad (30)$$

Comparing (29) and (30), we can find the upper bound on the convergence time as, $t \leq \frac{\|S(0)\|_2}{\sigma_{min}}$. ■

B. Sliding Phase

Theorem 2: For the system represented in (12), the corresponding sliding surface in (22) is asymptotically stable and satisfies (19) and hence the control objective in (9) and (10) during sliding phase.

Proof: During sliding phase $S = 0$,

$$(\mathcal{L} + I_{n_{\mathbb{a}}})\begin{bmatrix} s_i \\ \vdots \\ s_{n_{\mathbb{a}}} \end{bmatrix} = 0.$$

Since $(\mathcal{L} + I_{n_{\mathbb{a}}}) > 0$,

$$e_{2,i} + \lambda e_{1,i} = 0.$$

Since $\dot{e}_{1,i} = e_{2,i}$ with $\lambda \in \mathbb{R}_{>0}$, implies that, $e_{1,i} = 0$ and $e_{2,i} = 0$, $(\forall i \in N_{\mathbb{a}})$. So,

$$\chi_i - \tilde{\chi}_i^* = 0, \forall i \in N_{\mathbb{a}}. \quad (31)$$
$$\Rightarrow \chi = \chi^* \quad (32)$$

Equation (32) exists because (31) satisfies (19) collectively for the complete network and hence the control objective in (9) and (10). ■

V. Performance Analysis

The performance of the proposed control scheme is evaluated using a seven node MATLAB/Simulink model. The simulation is performed using DCSMC and DAI based *secondary* controls and performances are compared critically.

A. Simulation Model

The model contains five MRAs, $N_{\mathbb{a}} = \{n_1, \ldots n_5\}$ with local load $P_{LL} = \{0\ 0\ 0\ p_{LL,4}\ 0\}$ and two load-units; $N_L = \{n_6, n_7\}$, as shown in Figure 2. The MRAs are connected through inductive power lines and communication links. The per unit values of different parameters of the model are reported in the Appendix. The values of tuning parameters for DCSMC (λ, ψ, φ) and DAI (k_w, k_p) are selected via manual tuning. The values are reported in the Appendix, along with different parameters of the network.

B. Effect of Damping Coefficient

The per unit values of different parameters of the network (including the damping factor $D = \{1.6\ 1.22\ 1.38\ 1.42\ 1.30\}\ pu$) are obtained from [29]. Since the performance of DAI is largely affected by the value of damping factor (D) used in dynamic (12), different values of damping factor (multiple of D; $10D, 20D, 40D, 100D, 200D$) are used and the performance of both the control schemes are compared. The results of DAI obtained for different damping values are in accordance with classical control theory. Large values of D result in smaller frequency deviation (or over-shoot) and slower convergence to steady state, while the smaller values of D exhibit the oscillatory behavior. However, the DCMSC is unaffected by the choice of D and possess constant convergence time.

C. Step Change in Load

Figure 3 represents the total power demand $(p_{l,6} + p_{l,7} + p_{LL,4})$ of the network with abrupt changes at '1 second' and '3 seconds'. At a simulation time of '1 second', the load $p_{l,7}$ increases from $2.482\ pu$ to $4.86\ pu$, while the value of $p_{l,6}$ increases from $1\ pu$ to $2\ pu$ at simulation time of '3 seconds' causing fluctuations in frequency and power. The simulation starts with steady state values, the DAI control (11) and DCSMC (26) are used to achieve the control objectives in (9) and (10). Both the control schemes are analyzed at different values of damping factor.

1. Frequency Regulation

Figure 4 shows the frequency ($f_2 = 2\pi\omega_2$) of a single MRA (n_2) at different values of damping factor ($D, 10D, 20D, 40D$), for DAI control. Figure 4 represents large deviation, slow convergence and oscillations in frequency at a damping value of D. However, increasing the damping value significantly improves the performance of DAI. Increase in damping value decreases the magnitude of frequency deviation but reduces the convergence speed and the system takes a long time to reach the steady state. Figure 5 represents the response of DAI at significantly large damping values ($100D, 200D$), it shows a small deviation in frequency due to a disturbance at '1 second' and negligible deviation at '3 seconds'. However, large damping values result in proportionally slow convergence to steady state. Figures 6 and 7 represent the corresponding results of DCSMC. Both the Figures illustrate that the performance of DCSMC is not compromised at different damping values. The control possesses fast and identical convergence time for all damping values (even at damping values equal to D). The increase in damping value reduces the frequency overshoot, without affecting the convergence speed. In both the Figures the convergence time of DCSMC is less than '0.3 second'.

For DAI control the best choice for damping value in the presented simulation scenario is $20D$, where the control does not exhibit the oscillations (which are present in the case of D and $10D$) and possesses fast convergence (as compared to $40D$ and greater values). Figures 8 and 9 represent the frequency regulation of the complete network at a damping value of $20D$, for DAI and DCSMC respectively. The graphs illustrate active frequency regulation with small deviation. However, the DAI requires longer time (more than '2 seconds') to attain nominal frequency, after each disturbance. While in the case of DCSMC, all the MRAs converge to nominal frequency within '0.3 seconds'.

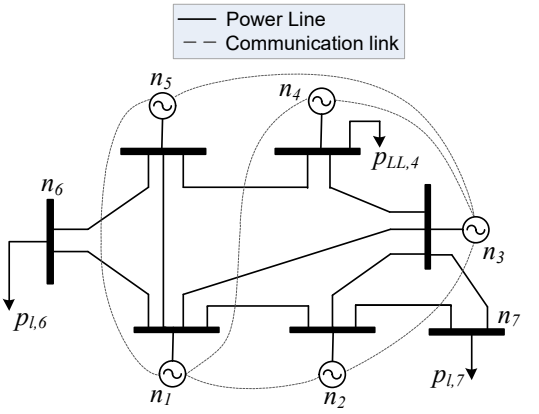

Figure 2. Seven node power network with inter-connecting power and communication lines.

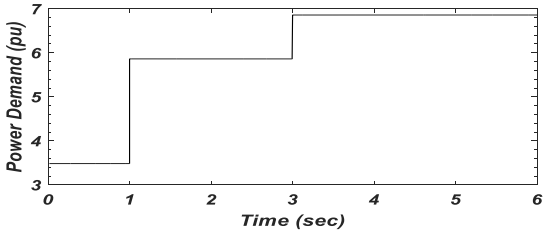

Figure 3. Total power demand

2. Identical Incremental Cost

The DAI is particularly slow in achieving the second control objective (10) that is, convergence to identical incremental cost. The convergence to identical incremental cost is analyzed at damping values of $100D$ and $20D$. Figure 10 presents the slow response of DAI at a damping value of ($100D$). The control fails to reach the identical incremental cost after both the disturbances. The performance of DAI improves at a damping value of $20D$, as represented in Figure 11. However, the control still consumes more than '2 seconds' to reach the identical incremental cost for both the disturbances.

The response of DCSMC, for $100D$ and $20D$ is represented in Figure 12 and Figure 13, respectively. Figure 12 and Figure 13 are almost identical and possess the same convergence time, which is less than '0.3 seconds'. Hence, the performance of DCSMC is unaffected by the choice of damping value.

The performance of DCSMC and DAI is summarized in Table 1. In Table 1, the DCSMC has comparatively greater

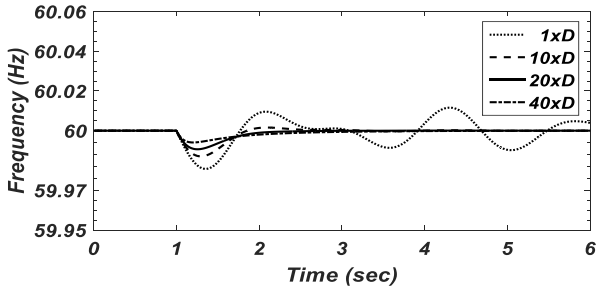

Figure 4. Instantaneous frequency of 2nd MRA at small values of damping-factor, with DAI control

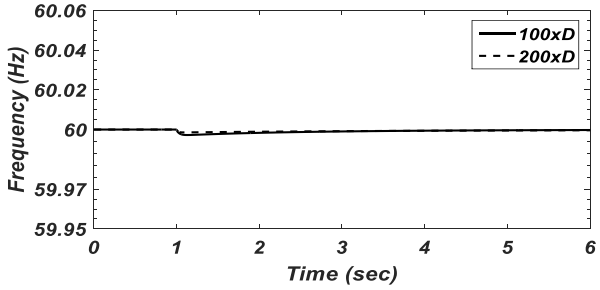

Figure 5. Instantaneous frequency of 2nd MRA at large values of damping-factor, with DAI control

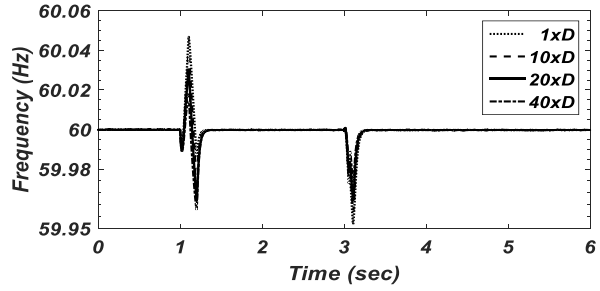

Figure 6. Instantaneous frequency of 2nd MRA at small values of damping-factor, with DCSMC control

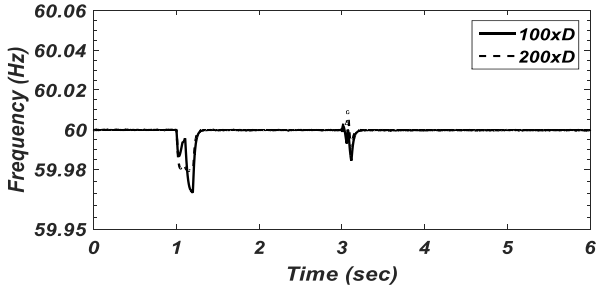

Figure 7. Instantaneous frequency of 2nd MRA at large values of damping-factor, with DCSMC control

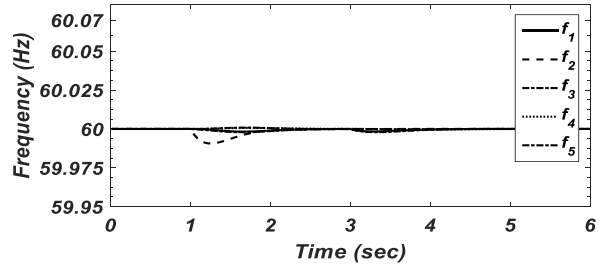

Figure 8. Instantaneous frequency (ω_i) of each MRA with DAI control

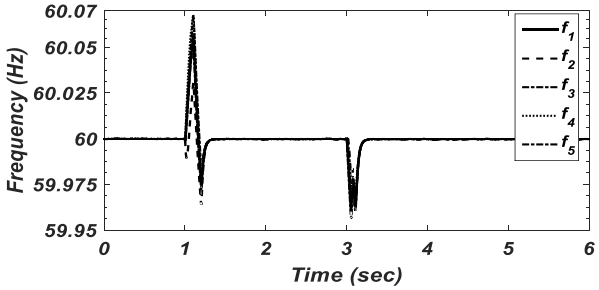

Figure 9. Instantaneous frequency (ω_i) of each MRA with DCSMC

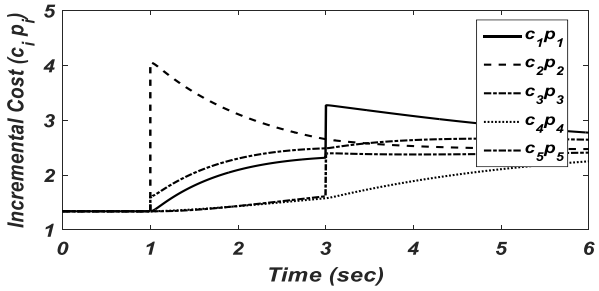

Figure 10. Incremental cost ($c_i p_i$) at $100D$ with DAI control

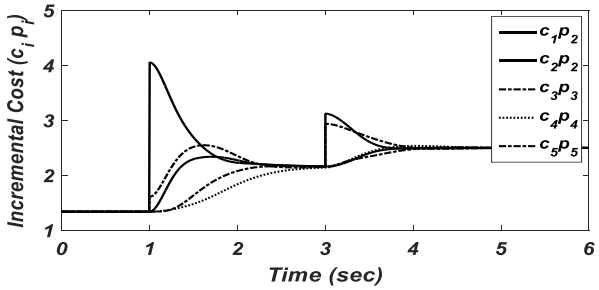

Figure 11. Incremental cost ($c_i p_i$) at $20D$ with DAI control

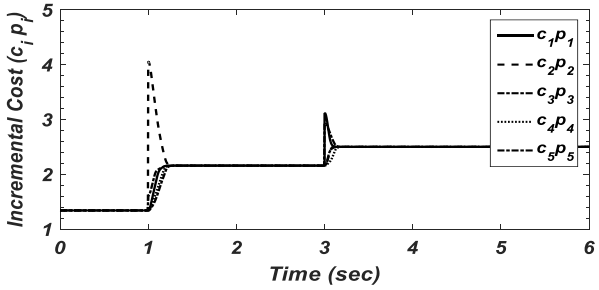

Figure 12. Incremental cost ($c_i p_i$) at $100D$ with DCSMC

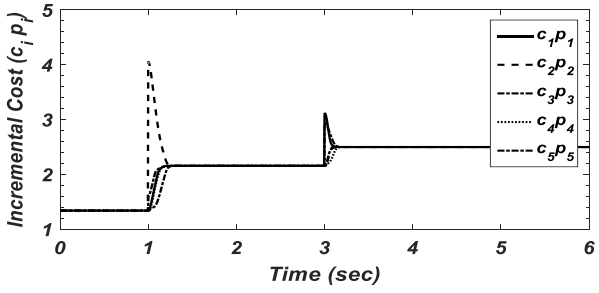

Figure 13. Incremental cost ($c_i p_i$) at $20D$ with DCSMC

Table 1. Performance Comparison of DAI and DCSMC at damping value of $20D$.

	Performance Parameters								
Control	Maximum Overshoot ($\Delta\omega$) (1 sec)	Maximum Overshoot ($\Delta\omega$) (3 sec)	Maximum Overshoot ($c_i p_i$) (1 sec)	Maximum Overshoot ($c_i p_i$) (3 sec)	Settling Time ($\Delta\omega$) (1 sec)	Settling Time ($\Delta\omega$) (3 sec)	Settling Time ($c_i p_i$) (1 sec)	Settling Time ($c_i p_i$) (3 sec)	IAE
DAI	0.0094	0.0021	1.897	0.6203	>2	2.4	>2	2.4	3.921
DCSMC	0.0677	0.0435	1.8967	0.6153	0.3	0.25	0.3	0.25	0.637

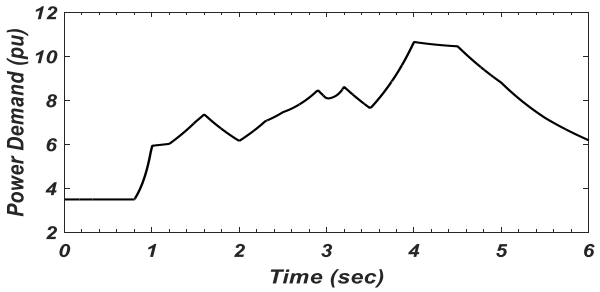

Figure 14. Continuously Varying Power Demand

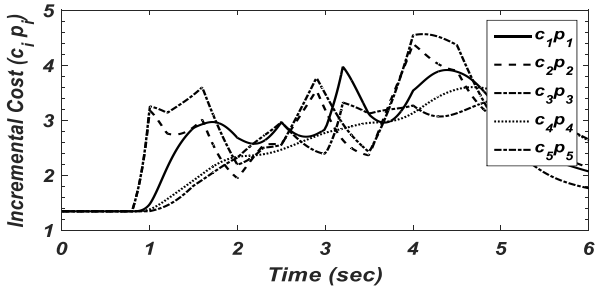

Figure 15. Incremental cost ($c_i p_i$) at $20D$ with DAI control

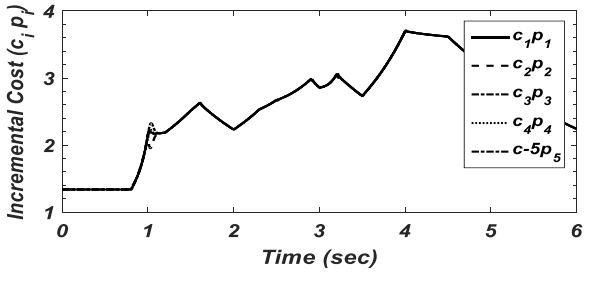

Figure 16. Incremental cost ($c_i p_i$) at $20D$ with DCSMC

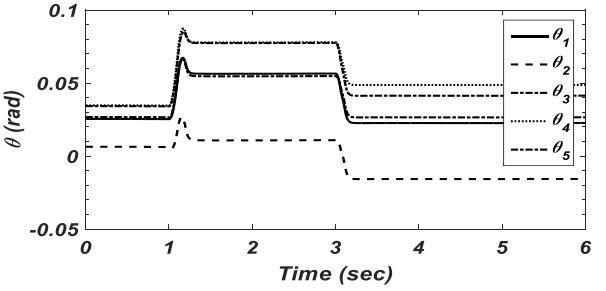

Figure 17. Instantaneous phase deviation with DCSMC

overshoot in frequency, however the overshoot values are well within the acceptable limit. Both the control schemes

possess identical overshoot values in incremental cost after applying both the disturbances. The performance of DCSMC is far superior in terms of fast convergence. The DCSMC has comparatively small settling time in both frequency and incremental cost curves. Finally, the performance index 'Integral Absolute Error' (IAE) is used to compare the performance of both the control schemes. The IAE is defined as;

$$IAE = \int_1^6 \sum|\Delta\omega|\, dt + \int_1^6 \sum|c_i p_i - \mathbb{c}^*|\, dt,$$

Where $\mathbb{c}^*$ represents the identical incremental cost value of the network, such that; $c_1 p_1^* = c_2 p_2^* = \cdots = c_{n_a} p_{n_a}^* = \mathbb{c}^*$. The IAE clearly illustrates the effectiveness of DCSMC the values are quite low as compared to DAI.

D. Continuously Varying Load

The performance of DCSMC is also tested for continuously varying power demand. Figure 14 presents the fluctuating power demand in the network. Due to the slow response, the DAI fails to converge to identical cost in the presence of fluctuating power demand, as shown in Figure 15. While the DCSMC in Figure 16, exhibits fast response and maintains ED in the system by forcing MRAs to operate at identical incremental cost.

E. Phase Deviation

Figure 17 illustrates the instantaneous phase deviation ($\Delta\theta$) of MRAs for DCSMC at a damping value of $20D$. The second order dynamics of primary control together with an increase damping value smooths out the chattering effect in control law (26). Hence, the chattering in DCSMC does not affect the power quality in the network.

F. Impact of DCSMC on ARG

The simulation results highlight the fast convergence of DCSMC in the presence of abrupt as well as continuous fluctuations in the power demand. The robustness of DCSMC to the choice of damping factor is also presented. While the DAI fails to maintain the ED in low inertia ARG with continuous fluctuations in power demand, resulting in

increased production cost. The comparative analysis highlights the superiority of DCSMC over conventional DAI control.

VI. Conclusion and Future Work

In this work, we considered an ARG with MRA to meet the power demand of the network. Being different in nature, the MRA operates the AC network by emulating the behavior of a synchronous generator with the help of associated control. This implies that the stability of ARG depends upon the efficiency of the control. In AC networks, stability of the system depends upon stability of frequency, which originates from the balance of active power. This assigns a prime importance to the role of *secondary* control providing frequency stabilization. Another aspect of the *secondary* control is to provide ED for cost effective optimum operation of the system. The DAI based secondary control displays a slow response to the non-linear dynamics of the system. This work proposes the use of DSMC based, non-linear technique to provide fast convergence, robustness and improved transient response. It stabilizes the frequency quite effectively, while providing the ED for cost reduction.

DCSMC is implemented as a local control on each MRA. At each MRA a distributed sliding surface is formed with the help of local measurement and communication with the neighboring MRAs. The MRAs calculate the intermediate optimum state values and force the local states to track them. The intermediate optimum states are continuously updated and ultimately lead (asymptotically) to the global optimum point. The convergence and stability of the proposed control is proved analytically, while the performance is evaluated with the help of MATLAB/Simulink based simulation and a comparison with DAI control.

The possible extensions to the presented work include analysis of DCSMC for communication delays, link failures, and dynamic (power and communication) network topologies. The proposed control scheme can also be used for the other aspect of secondary control that is voltage regulation and reactive power distribution.

REFERENCES

[1] Jing Qiu, Zhao Xu, Yu Zheng, Dongxiao Wang, "Distributed generation and energy storage system planning for a distributed system operator", *IET Renewable Power Generation,* vol. 12, no. 12, 2018.

[2] S.C.E. Jupe, P.C. Taylor, A. Michiorri, " Coordinated output control of multiple distributed generation schemes", *IET Renewable Power* Generation, vol. 4, no. 3, 2010.

[3] Fyali Jibji-Bukar, Olimpo Anaya-Lara, "Frequency support from photovoltaic power plants using offline maximum power point tracking and variable droop control", IET Renewable Power Generation, vol. 13, no. 13, 2019.

[4] Md A. Hossain, H. R. Pota, W. Issa, Md J. Hossain, "Overview of AC Microgrid Controls with Inverter-Interfaced Generations", *energies*, 2017, doi: 10.3390/en10091300.

[5] Moushumi Patowary, Gayadhar Panda, Bonu Ramesh Naidu, "ANN-based adaptive current controller for on-grid DG system to meet frequency deviation and transient load challenges with hardware implementation", *IET Renewable Power Generation,* vol. 12, no. 1, 2018.

[6] Olve Mo, S. D'Arco, J.A. Suul, "Evaluation of Virtual Synchronous Machines With Dynamic or Quasi-Stationary Machine Models" *IEEE Transaction on Industrial Electronics,* vol. 64, no. 7, 2017, doi: 10.1109/TIE.2016.2638810.

[7] I. Ziouani, D. Boukhetala, A. M. Darcherif, B. Amghar, Ikram El, "Hierarchical control for flexible microgrid based on three-phase voltage source inverters operated in parallel", *International Journal of Electrical Power & Energy Systems*, vol. 95, February 2018.

[8] F. Anwaar, N. Iltaf, H. Afzal, R. Nawaz, "HRS-CE: A hybrid framework to integrate content embeddings in recommender systems for cold start items", *Journal of Computational Science*, vol. 29, no. 1, pp. 9-18, Nov. 2018.

[9] Josep M. Guerrero, Juan C. Vasquez. "Hierarchical Control of Droop-Controlled AC and DC Microgrids—A General Approach Toward Standardization". *IEEE Transactions on Industrial Electronics*, vol. 58, no. 1, 2011.

[10] John Simpson-Porco, Qobad Shafiee, "Secondary Frequency and Voltage Control of Islanded Microgrids via Distributed Averaging", *IEEE Transactions on Industrial Electronics*, vol. 62, no. 11, 2015.

[11] C. Zhao, E. Mallada, F. Dorfler, "Distributed Frequency Control for Stability and Economic Dispatch in Power Networks", *American Control Conference,* 2015.

[12] F. Dorfler, J. W. Simpson-Porce, F. Bullo, "Breaking the Hierarchy: Distributed Control & Economic Optimality in Microgrids" *IEEE Transaction on Control of Network System,* vol. 3, no. 3, 2016, doi: 10.1109/TCNS.2015.2459391.

[13] Johannes Schiffer a, Florian Dörfler, "Robustness of distributed averaging control in power systems: Time delays & dynamic communication topology". *Automatica* 80 (2017) 261–271.

[14] L. Meng, Mehdi S., F. Andrade, "Microgrid Central Controller Development and Hierarchical Control Implementation in the Intelligent MicroGrid Lab of Aalborg University", *Proc. IEEE APEC,* 2015.

[15] Zaheeruddin, M. Manas, "Renewable energy management through microgrid central controller design: An approach to integrate solar, wind and biomass with battery", *Energy Report,* (156 – 163), 2015.

[16] A. Tuckey, S. Sabihi, S. Round, "Decentralized control of a microgrid", *European Control Conference on Power Electronics and Applications,* 2017, doi: 10.23919/EPE17ECCEEurope.2017.8098969.

[17] G. Lou, W. Gu, L. Wang, Bin Xu, Ming Wu, W. Sheng, "Decentralized secondary voltage and frequency control scheme for islanded microgrid based on adaptive state estimator" *IET Generation, Transmission & Distribution,* vol. 11, no. 15, 2017.

[18] W. Liu, W. Gu, Y. Xu, "General distributed secondary control for multi-microgrids with both PQ-controlled and droop-controlled distributed generators", *IET Generation, Transmission & Distribution*, vol. 11, no. 13, 2017.

[19] Ananiadou, Sophia, P. Thompson, and R. Nawaz. "Enhancing search: Events and their discourse context." In International Conference on Intelligent Text Processing and Computational Linguistics, pp. 318-334. Springer, Berlin, Heidelberg, 2013.

[20] Johannes Schiffer and Florian Dörfler, "On Stability of a Distributed Averaging PI Frequency and Active Power Controlled Differential-

Algebraic Power System Model", *European Control Conference (ECC), Aalborg, Denmark*, 2016.

[21] Andreasson, M., Sandberg, H., Dimarogonas, D.V., & Johansson, K.H. "Distributed integral action: Stability analysis and frequency control of power systems". *IEEE conference on decision and control* Maui, HI, USA (pp. 2077–2083), 2012.

[22] Simpson-Porco, J. W., Dörfler, F., & Bullo, F. "Synchronization and power sharing for droop-controlled inverters in islanded microgrids". *Automatica*, 49(9), 2603–2611, 2013.

[23] R.A. Freeman, P. Yang, "Stability and Convergence Properties of Dynamic Average Consensus Estimators" 45th *IEEE Conference on Decision & Control* Manchester USA, December 13-15, 2006.

[24] H. Flamme, E. Tegling, H. Sandberg, "Performance Limitations of Distributed Integral Control in Power Networks Under Noisy Measurements", *Optimization and Control (math.OC), American Control Conference,* 2018.

[25] Oureilidis, Konstantinos O., E. A. Bakirtzis, and Charis S. Demoulias. "Frequency-based control of islanded microgrid with renewable energy sources and energy storage." Journal of Modern Power Systems and Clean Energy 4, no. 1 (2016): 54-62

[26] Qadir, Hajra, O. Khalid, Muhammad US Khan, A. U. Rehman Khan, and R. Nawaz. "An Optimal Ride Sharing Recommendation Framework for Carpooling Services." IEEE Access 6 (2018): 62296-62313.

[27] Y. Zheng, S. Eben Li, K. Li, F. Borrelli, "Distributed Model Predictive Control for Heterogenous Vehicle Platoons under Unidirectional Topologies", *IEEE Transactions on Control Systems Technology* vol. 25, Issue. 3, 2017.

[28] Yujia Wu1, Shengbo Eben Li, **"**Distributed Sliding Mode Control for Multi-vehicle Systems with Positive Definite Topologies", 2016 *IEEE 55th Conference on Decision and Control (CDC)* ARIA Resort & Casino, 2016.

[29] S. Trip, M. Burger, C. D. Persis, "An internal model approach to (optimal) frequency regulation in power grids with time-varying voltages", *Automatica*, vol 64, 240-253, 2016.

Appendix

The per unit values of parameters related to network and MRAs are obtained from [29] and are listed below.

$\{d_1\ d_2\ d_3\ d_4\ d_5\} = \{1.6\ 1.22\ 1.38\ 1.42\ 1.30\}\ pu.$

$\{m_1\ m_2\ m\ m_4\ m_5\} = \{5.22\ 3.98\ 4.49\ 4.22\ 5.4\}\ pu.$

$\{b_{12}\ b_{13}\ b_{23}\ b_{34}\ b_{45}\ b_{51}\} = \{64.7\ 61.51\ 58.75\ 51.7\ 54.7\ 62\}\ pu,$

$\{b_{16}\ b_{56}\ b_{27}\ b_{37}\} = \{50.9\ 55.26\ 56.31\ 2.95\}\ pu,$

$\{P_{l,6}\ p_{l,7}\} = \{2.482\ 1\},\ p_{LL,4} = 0.4167\ pu,$

$\{v_1\ v_2\ v_3\ v_4\ v_5\} = \{1\ 1\ 1\ 1\ 1\}\ pu.$

The cost rate of with each MRA is given below,

$\{c_1\ \ c_2\ c_3\ c_4\ \ c_5\} = \{2\ \ 1.2\ 2.3\ 2.1\ 1.5\}\ pu.$

Tuning parameter of DAI and DCSMC.

$\{K_p\ K_w\ \} = \{500\ 2000\}, \{\varphi\ \psi\ \lambda\} = \{1\ 1\ 50\}.$